ISSN 2277-2685

IJPSL/May . 2022/ Vol-12/Issue-2/1-10

Mercy florence *et. al* International Journal of Pharmacetical Sciences Letters

The Cytotoxic Effects of Surfactant-Mediated Noble Metal Nanoparticle Synthesis on Breast Cancer Cells

Mercy florence, Ch. Sushma ,G.Ratnakumari, Mohammad afrah

ABSTRACT

The biomedical applications of the noble metal nanoparticles have been the field of interest, especially in cancer therapy. In this paper, the synthesis of spherical silver and gold nanoparticles and their apoptotic activity against breast cancer cells is reported. The chemicals reduction method is used to synthesize nanoparticles. Two different types of surfactants i.e., citrate and polyvinylpyrrolidone were used as a reducing and capping agent. The synthesized nanoparticles have been characterized using X-ray diffraction, ultraviolet-visible absorption spectroscopy, dynamic light scattering, zeta potential and transmission electron microscopy. The synthesized nanoparticles have crystalline phase with average size in the range of 25-30 nm and possess negative surface charge. In vitro studies of nanoparticles against breast cancer cells (MCF-7), were performed. The results show the significant cytotoxicity of nanoparticles against the cancer cell line and found to be mediated by DNA damage.

Key words: Breast cancer cell line (MCF-7), deoxyribonucleic acid damage, metal nanoparticles, poly vinyl pyrrolidone, silver nanoparticles, trisodium citrate

INTRODUCTION

As the leading killer on a global scale, cancer affects people's financial stability, quality of life, and access to healthcare. Anticancer drugs such vinblastine, doxorubicin, taxol, and cisplatin, among others, are more effectively delivered to all disease sites, including micro metastatic lesions, during chemotherapy compared to radiation and surgery [1,2]. Systematic administration of cytotoxic medicines during chemotherapy is now plagued by two main difficulties. Two factors must be considered: first, the dosage-limiting toxicity to healthy tissues, and second, the patient's innate or acquired multidrug resistance. Nanomaterials have recently gained a lot of attention for their possible utility in medicine, both in diagnosis and treatment [3-5]. The possibility to deliberately alter the physico-chemical and biological properties of silver and gold nanoparticles, as well as recent breakthroughs in synthesis, have created new possibilities for nano-medicine applications [6,7]. Important variables include the reactants, pH, temperature, mixing order, presence of

electrophilic and nucleophilic reagents, stabilizer type, and rate of reducing agent addition in the experiment [8–10]. These factors impact the physicochemical characteristics, color, stability, shape, and size of nanoparticles made of advanced nanomaterials [11]. Natural and synthetic ligands or polymers are often used as protective or capping agents to avoid aggregation during the synthesis and production of metal nanoparticles [12,13]. Because the nature of the reducing agent affects the size, shape, and distribution of particle sizes, selecting an appropriate reducing agent is also crucial. The metal precursor is decreased when a reducing agent is introduced [14].

The exceptional characteristics of metal nanoparticles from noble metals like silver and gold, including surface enhanced Raman scattering, high conductivity, catalysis, and antibacterial effect, as well as their uses in electronics, bio-labeling, and catalysis, have attracted a great deal of research attention [15–18]. Noble nanomaterials exhibit strong optical field increases due to the resonant oscillation of their free electrons when exposed to light. Optics, imaging, sensing, cosmetics, cancer treatment, and medicine delivery are just a few of the many fields that benefit from the special properties of noble metal nanoparticles [19–21]. It is possible to synthesize metal nanoparticles under mild and uncomplicated circumstances. Applying a stabilizing layer such as Cetyltrimethylammonium Bromide (CTAB), Polyvinyl Alcohol (PVA), cyclodextrin, poly (methylhydrosiloxane), or Polyvinylpyrrolidone (PVP) enables the use of common reducing agents such as sodium borohydride, hydrazine, sodium citrate, thiols, amino acids, and polyols [13,14,22-26]. PVP is a

hydrophilic polymer that is also kind to the environment. One interesting approach to making nanoparticles with tailorable optical characteristics and morphologies is to coat them with polymers like PVP. Using trisodium citrate and PVP as capping agents, we aim to produce silver and gold nanoparticles in this work. In order to learn how various nanoparticles with surfactant caps interact with breast cancer cells, researchers have conducted a comparative study.

MATERIALS AND METHODS

Materials:

Sodium borohydride (NaBH4), silver nitrate (AgNO3), trisodium citrate (Na3C6H5O7), polyvinylpyrrolidone (PVP), and hydrochloroauric acid (HAuCl4.3H2O) were all purchased from Sigma Aldrich Chemicals.

Methods:

Nanoparticles of trisodium citrate encased in gold: To create AgNPsC, or silver nanoparticles with a citrate cap, a solution of AgNO3 (1 mM, 50 ml) was heated and swirled using a magnetic stirrer's hot plate. Afterwards, while stirring continuously, 1% tri sodium citrate solution was added drop by drop to the boiling solution. The synthesis of AgNPsc is shown by the absorption of a dark yellow color. As a reducing and capping agent, tri-sodium citrate is useful [27].

Hydrochloroauric acid (HAuCl4.3H2O) (1 mM, 50 ml) was produced for the manufacture of citrate capped gold nanoparticles (AuNPsC) in deionized water. After that, a solution of HAuCl4.3H2O in 50 ml was heated while being agitated constantly. Step by step, when the solution came to a boil, a water-based tri-sodium citrate (C6H5Na3O7) solution (1% w/w, 5 ml) was added to the boiling mixture. As AuNPsc formed, the solution took on a reddish-wine hue. As an agent for both reduction and stabilization, tri-sodium citrate is useful[27,28]. The synthesis of AgNPsc and AuNPsc is shown in Fig. 1, which is a flow diagram.

Using NaBH4 (2 mM, 30 ml) as a reducing agent and PVP (0.3 %, 100 µl) as a stabilizing agent, PVP capped silver nanoparticles (AgNPsPVP) and gold nanoparticles were created. The ice-cold NaBH4 solution was supplemented with an aqueous AgNO3 solution. It was added to the solution as soon as the color changed to PVP. The synthesis of AgNPsPVP is shown in Fig. 1, which is a flow diagram. The starting solution for the synthesis of AuNPsPVP was a water-based HAuCl4.3H2O solution (1 mM, 50 ml). In order to extract Au3+ ions, the solution was heated to 100 ° for 30 minutes. By introducing 2 mM of NaBH4, these Au3+ ions were decreased. At the conclusion of the reaction, add 100 µl of 1% PVP to prevent the solution from clumping together. The synthesis of AuNPsPVP is shown in Fig. 1, which is a flow diagram.

Characterization:

Ultraviolet (UV)-visible absorption spectroscopy: The materials were scanned in the 300-700 nm range using a LABINDIA UV-3000+ spectrometer to examine optical absorption spectra. The creation of AgNPs and AuNPs, respectively, is indicated by the existence of plasmon resonance (SPR) peaks at 420 and 520 nm. Utilizing Cu Kα (0.15406 nm) radiation, the X' Pert PRO X-Ray diffractometer captured the X-Ray diffraction pattern of AgNPs and AuNPs. Through the process of drop casting, the film was applied on pristine glass slides. The range was set at 2θ=35° to 80° and the scanning speed was set at 5°/min. Atomic Force Microscopy (AFM): Through transmission electron microscopy, the size and morphology of the particles were studied. For the ultra-structural assessment of produced nanoparticles, a transmission electron microscope (TEM) with a charge-coupled device camera and a voltage of 120 kV was used (Hitachi H-7500, Japan). With an operating voltage range of 40-120 kV, this device can magnify objects up to 600,000 times in high resolution mode and boasts a high resolution of 0.36 nm. Through transmission electron microscopy, the size and morphology of the particles were studied. The zeta potential and dynamic light scattering: Using a Malvern zetasizer (ZEN3600), the researchers investigated the zeta potential and size distribution of AgNPs and AuNPs. Particle size distributions of AgNPsC, AgNPsPVP, AuNPsC, and AgNPsPVP were investigated using Dynamic Light Scattering (DLS). From nanometers to a few micrometers, DLS measures a broad range of hydrodynamic diameters.

Research on cytotoxicity:

Culture of cells: Cancer of the breast The MCF-7 cells were maintained in a humidified environment with 5% CO2 and 10% FBS in a continuous culture of Eagles MEM at 37°. Replacement of the media occurred every 48 hours. The confluent monolayer of MCF-7 cells was separated by spinning at 200 ×g for 2 minutes with trypsin (0.25%)-ethylenediaminetetraacetic acid (0.02% in PBS), then washed with serum-free media. The washed pellet was carefully mixed with 5 ml of complete medium Eagle's MEM in a T25 flask. The mixture was then incubated at 37° with 5% CO2 to facilitate further processing. To test for cytotoxicity, we cultivated the cells overnight in a CO2 incubator with humidified conditions after routinely cultivating them; we used 10,000 cells per well in our 96-well plate. Various quantities of AgNPs and AuNPs, as well as the conventional chemotherapeutic medication palbociclib, were added to cells after 24 hours for varying durations of treatment. The cells were treated with 3-[4,5-dimethylthiazol-2-yl]-2,5 diphenyl tetrazolium bromide (MTT) and then incubated in a CO2 incubator for 4 hours following the corresponding treatment time intervals. Subsequently, DMSO was used to dissolve the formazan crystals, and a plate reader was used to measure absorbance at 532 nm in order to determine cytotoxicity.

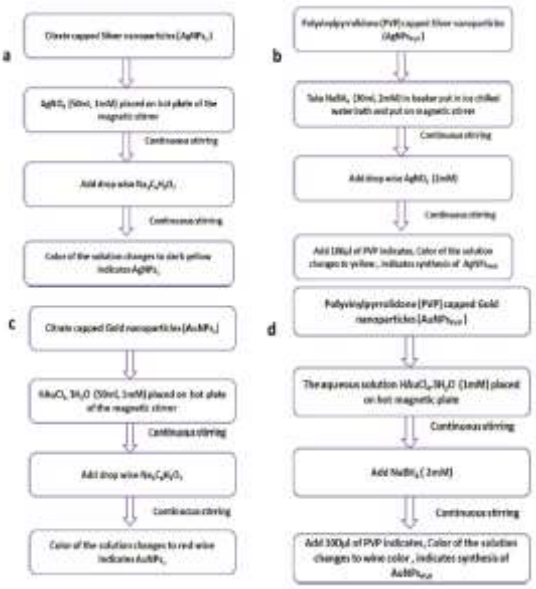

Fig. 1: Flowchart for synthesis of (a) AgNPsC; (b) AgNPsPVP; (c) AuNPsC and (d) AuNPsPVP

Structural changes by microscopy:

The morphology of the treated cells was examined using a phase contrast microscope in order to analyze the structural changes generated by metallic nanoparticles. The cells were treated with varying concentrations and time intervals. Assessment of apoptotic activity caused by palbociclib, AgNPs, and AuNPs was done using fluorescent microscopy. Researchers subjected cells to a series of treatments, including metallic nanoparticles, ethidium bromide, and acridine orange, to measure the degree of DNA damage and micronuclei production, respectively.

RESULTS AND DISCUSSION

The absorption spectra of silver and gold nanoparticles in the UV-visible range are shown in Figure 2. Typically, in the visible portion of the electromagnetic spectrum, spherical AgNPs will exhibit an SPR peak between 400 and 450 nm, while AuNPs will do the same between 500 and 550 nm. At 420 nm, 525 nm, 431 nm, and 520 nm, respectively, the absorption spectra reveal the SPR peak of AgNPsC, AuNPsC, AgNPsPVP, and AuNPsPVP. From figure 2, it is clear that the SPR peaks of AgNPs and AuNPs vary when it comes to PVP and citrate capping agents. This is because surfactant and nanoparticle interaction mechanisms are fundamentally different. Citrate is an anionic compound, while PVP is cationic. Trisodium citrate serves as both a reducing agent and a capping agent for AgNPsC and AuNPsC nanoparticles in the conventional chemical reduction technique. As the process progresses, the atoms undergo reduction, which causes them to nucleate in small

clusters that eventually form particles. Altering the precursor to reducing agent ratio allows one to regulate the size and structure of nanoparticles by regulating the quantity of atoms available for the process [27]. In order to stabilize AgNPs and AuNPs, the anionic component of citrate engages in an electrostatic stabilization process. The steric stabilizing mechanism of PVP, a water-soluble polymer, is widely used in the manufacture of stable nanoparticles of gold and silver. Both the nitrogen atom and the carbon atom in PVP are highly reactive, allowing the compound to react with a wide variety of compounds [29,30]. The stabilizing substance PVP interacts with the surfaces of silver and gold via the nitrogen atom.

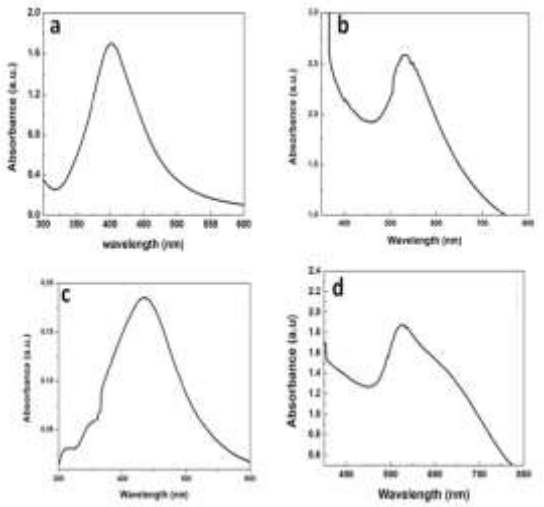

Fig. 2: The UV-Visible absorption spectra of (a) AgNPsC; (b) AuNPsC; (c) AgNPsPVP and (d) AuNPsPVP nanoparticles

The crystalline structure of the generated AgNPsC, AgNPsPVP, AuNPsC, and AuNPsPVP was examined using XRD measurements. Drop casting the material onto a glass substrate produced the thin film upon which the diffraction pattern was recorded. In Figure 3, we can see the XRD pattern of AgNPsC, AgNPsPVP, AuNPsC, and AuNPsPVP, in that order. The crystal planes of the face-centered cubic structure are (111), (200), (220) and (311), respectively, and the major peaks for AgNPsC, AgNPsPVP, AuNPsL, AuNPsC, and AuNPsPVP were observed at 2θ values of 38°, 44.2°, 64.3°, 77.3°, 38.03°, 45.1°, 63.9°, 77.4°; 37.9°, 44.4°, 64.3°, 77.4°; and 38.1°, 45.2°, 64.4°, 77.2°. Compared to the standard values in JCPDS files 04-0783 and 87-0717, these findings are in the same ballpark [31,32]. Using Debye Scherer's method, we were able to determine the average size of the crystals.

$$D=k\lambda/(\beta \cos\theta)$$

In this context, k represents Debye's constant, β corresponds to the full width half maximum (FWHM), θ denotes the diffraction angle, and λ represents the wavelength. Table 1 provides the numbers for the average crystalline size and the fraction of the reflection line.

As shown in Figure 4, the size distribution of AgNPsC, AgNPsPVP, AuNPsC, and AgNPsPVP is shown. The DLS results showed that the produced AgNPs and AuNPs containing different surfactants exhibited polydispersity. The degree to which an aqueous sample aggregates or the distribution of its sizes may be measured by the Polydispersity Index (PdI). It may take on values between zero and one in the zetasizer program. Samples with a lower PdI value are clearly monodisperse, in contrast to the more polydisperse character of samples with a higher PdI value. In terms of hydrodynamic average size, the following materials were considered: AgNPsC (38 nm), AuNPsC (40 nm), AgNPsPVP (44 nm), and AuNPsPVP (43 nm). It takes particles in aqueous solution with Brownian motion and treats them like a hard sphere to determine their hydrodynamic radius. In order to determine the charge on the particles, scientists measured their zeta potential, as shown in figure 5, for AgNPsC, AuNPsC, AgNPsPVP, and AuNPsPVP. Among the many possible configurations, we find zeta potentials of -20.1 mV for AgNPsC AuNPsC, -19.2 mV for AgNPsPVP, -16.9 mV

for AuNPsPVP, and -12.3 mV for AuNPsPVP. The long-term stability of the synthesized particles is supported by the negative zeta potential values of the AgNPsC, AgNPsPVP, AuNPsC, and AgNPsPVP dispersions.

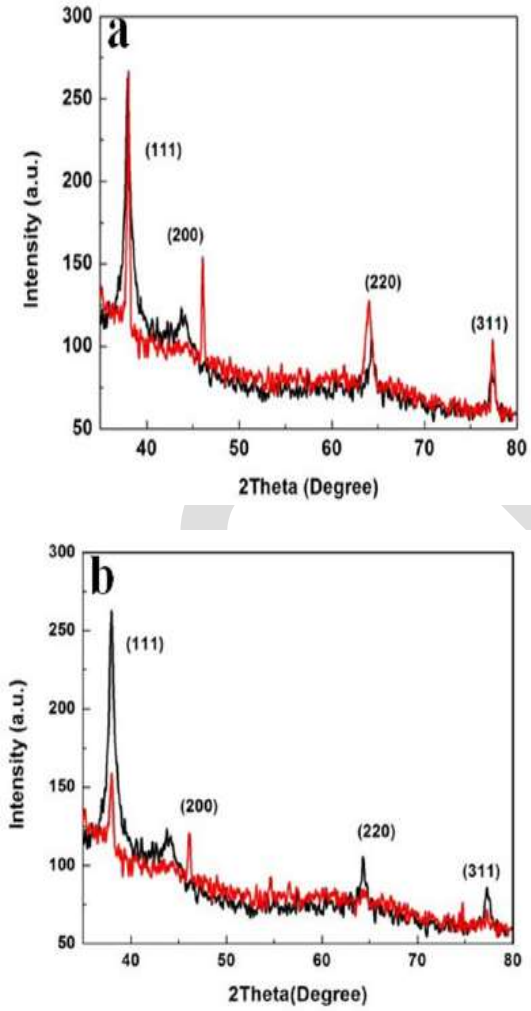

Fig. 3: XRD pattern of (a) AgNPsC and AgNPsPVP and (b) AuNPsC and AuNPsPVP recorded

TABLE 1: THE STRUCTURAL AND HYDRODYNAMICS PARAMERTERS OF SYNTHESIZED NANOPARTICLES

Plane/ material	(111)	(200)	(220)	(311)	Average crystalline size	DLS	PdI	Zeta potential	TEM
AgNPsPVP	38.03°	45.1°	63.9°	77.4°	~ 28 nm	44 nm	0.39	-16.9 mV	30 nm
AgNPsC	38°	44.2°	64.3°	77.3°	~10 nm	38 nm	0.64	-28.1 mV	25 nm
AuNPsC	37.9°	44.4°	64.3°	77.4°	~9 nm	48 nm	0.32	-19.2 mV	25 nm
AuNPsPVP	38.1°	45.2°	64.4°	77.2°	~21 nm	43 nm	0.958	-12.3 mV	31 nm

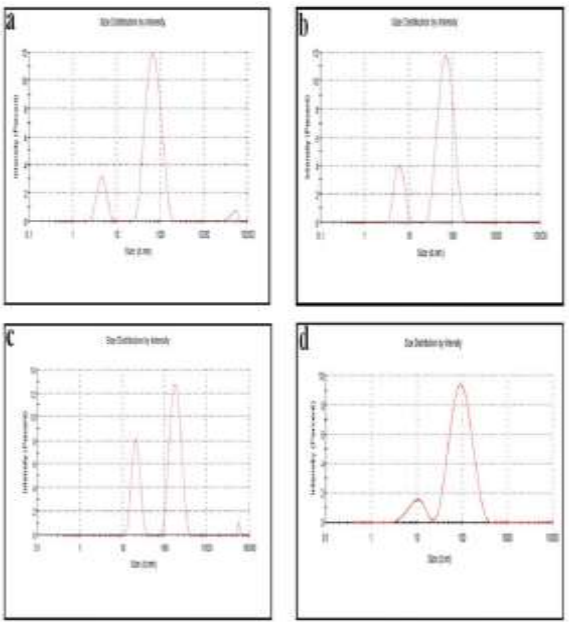

Fig. 4: The size distribution intensity for (a) AgNPsC, (b) AgNPsPVP, (c) AuNPsC and (d) AuNPsPVP

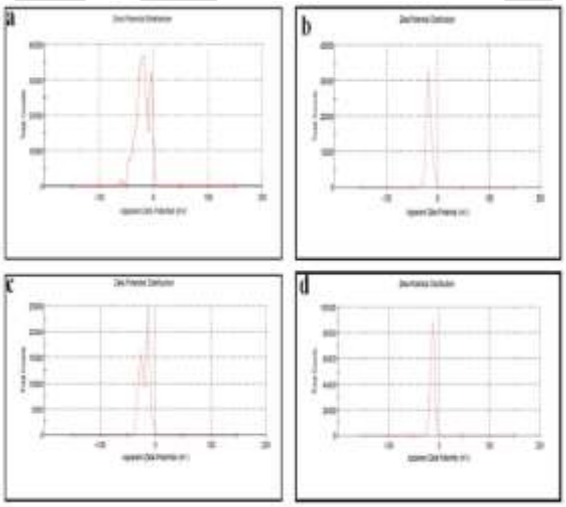

Fig. 5: Zeta potential of (a) AgNPsC; (b) AgNPsPVP; (c) AuNPsC and (d) AuNPsPVP

Figure 6 displays a transmission electron micrograph of AgNPsC, AgNPsPVP, AuNPsC, and AuNPsPVP. The TEM analysis showed that the particles were 20–35 nm in size and had a spherical shape. On average, the size of the particles was 25 nm for AgNPsC, 30 nm for AgNPsPVP, 25 nm for AuNPsC, and 31 nm for AuNPsPVP. The particles that come out of it are evenly scattered and not clumped together. The size acquired by DLS for the same AgNPsC, AgNPsPVP, AuNPsC, and AuNPsPVP was larger than the size measured by TEM. However, transmission electron microscopy (TEM) shows that the AgNPsC, AgNPsPVP, AuNPsC, and AuNPsPVP suspensions are dry and shrunk, in contrast to the wet and increased hydrodynamic diameter shown by differential scanning laser spectroscopy (DLS)[33].

Treatment with AgNPsC, AgNPsPVP, AuNPsC, and AuNPsPVP is uniform, but after 48 hours, the nanoparticles have accumulated, according to optical microscopy of the different nanoparticles treated for that length of time. It is evident that the MCF-7 cells are evenly dispersing and absorbing the smaller, non-

aggregated nanoparticles. When compared to normal, untreated cells, cells that have absorbed the nanoparticles exhibit structural alterations. Similar cellular structural changes as contrasted to normal cell morphology may be seen with the typical chemotherapy medication palbociclib. The MTT test was used to further assess the impact of these different nanoparticles on the cell viability. At 24 and 48 hours after treatment with different doses of the conventional chemotherapeutic medication, as well as AgNPsC, AgNPsPVP, AuNPsC, and AuNPsPVP, Fig. 7 displays the cell viability analysis using the MTT test of breast cancer cells. The cell viability was not significantly affected by lower doses according to the MTT findings, in comparison to doses at or beyond 20 µl/well (fig. 7a and fig. 7b). The aforementioned nanoparticles, however, considerably decreased cell viability, with reductions ranging from 22% to 33% (fig. 7a). The viability of the cells was further diminished as the time increased in the dosage range of 20-40 µl/well (fig. 7b). The usual chemotherapeutic treatment and these nanoparticles both diminish cell viability to a similar extent up to dosages of 20 µl/well. However, at higher doses, palbociclib considerably lowers cell viability even farther than the groups treated with nanoparticles. Both figures 7a and 7b show that citrate, not the PVP-coated nanoparticles of either metallic nanoparticle, has the most harmful effects of the two silver nanoparticles. It was possible to see that the nanoparticles had a cytotoxic impact on the breast cancer cells, similar to the usual chemotherapy medication up to certain levels, using optical microscopy and the MTT test. The effects of DNA damage were further investigated further by conducting fluorescence microscopy tests using acridine orange and ethidium bromide. The capacity of acridine orange to attach to viable cells and the ability of ethidium to bind to DNA after cell injury are well-established. Figure 8 displays fluorescent microscopy pictures of DNA damage treated with palbociclib medication and different nanoparticles. The photos clearly show that the cells treated with nanoparticles and chemotherapeutic drugs exhibit a more pronounced reddish-brown staining compared to the normal cells. This suggests that these agents exhibit cytotoxic action that damages DNA (fig. 8). The spherical nanoparticles with sizes ranging from 20-35 nm, as observed in TEM and DLS analysis, exhibit a strong cytotoxic effect through DNA damage, similar to that seen in chemotherapeutic drug treatment, and are thus synthesized from silver and gold nanoparticles using various agents. Numerous studies have shown that in this size range, different cell types efficiently and readily absorb nanoparticles [34]. This work and others like it have shown that, when compared to the gold standard chemotherapeutic medication, nanoparticles coated with citrate and PVP have distinct aggregation abilities once taken up by cells and, as a result, varied cytotoxic qualities. Nanoparticles of gold and silver may, therefore, have therapeutic promise as nanotherapeutics for the treatment of cancer.

The researchers in this work used polyvinylpyrrolidone (PVP) and trisodium citrate (TC) to create colloidal nanoparticles of gold and silver. In the UV-visible absorption spectra, the presence of SPR peaks verifies the production of spherical nanoparticles. The morphology of the various surfactant nanoparticles was shown to be spherical, crystalline, face-centered cubic, and very stable by means of a negative zeta potential value, according to DLS, TEM, XRD, and Zeta potential. Researchers have shown that nanoparticles have a cytotoxic impact, alter cellular shape, and are on par with the gold standard chemotherapeutic medication palbociclib in terms of how cells absorb and use these particles. When comparing AgNPsPVP, AgNPsC, and AuNPsPVP at different doses, it becomes clear that AgNPsPVP exhibits the highest cytotoxicity. Even more promising as nanotherapeutic agents for cancer therapy, these nanoparticles cause DNA damage in breast cancer cells via cytotoxicity, much like the chemotherapeutic medication.

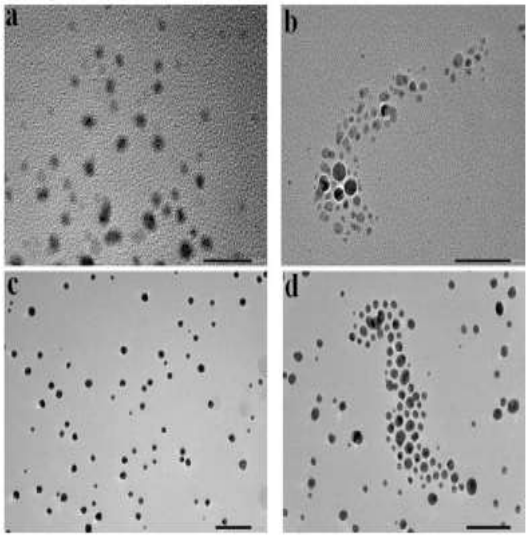

Fig. 6: The TEM micrographs of (a) AgNPsC; (b) AgNPsPVP; (c) AuNPsC and (d) AuNPsPVP

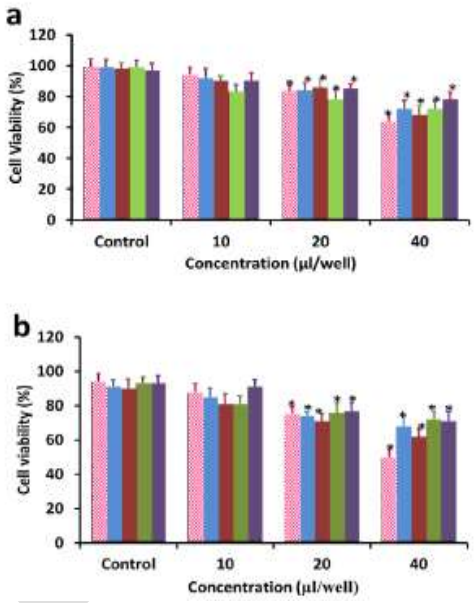

Fig. 7: Cell viability bar graph for MTT assay studies of different surfactant coated silver and gold nanoparticles on breast cancer cells (MCF-7) for 24 h (a) and 48 h (b); On the x-axis the concentration 10, 20 and 40 for palbociclib should be read as 10, 20 and 40 µM respectively

Note: (▒): Palbociclib; (▒): $AgNPs_C$; (▒): $AgNPs_{PVP}$; (▒): $AuNPs_C$ and (▒): $AuNPs_{PVP}$

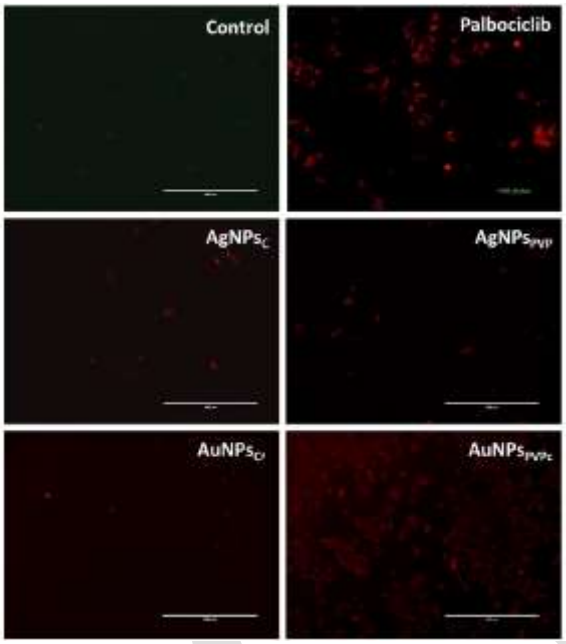

Fig. 8: DNA damage of the Breast cancer (MCF-7) cells changes using fluorescence microscopy (stained with ethidium bromide) at 48 h duration

REFERENCES

Akram M, Iqbal M, Daniyal M, Khan AU. Awareness and current knowledge of breast cancer. Biol Res 2017;50:23-50.

Klement G, Huang P, Mayer B, Green SK, Man S, Bohlen P, et al. Differences in therapeutic indexes of combination metronomic chemotherapy and an anti-VEGFR-2 antibody in multidrug-resistant human breast cancer xenografts. Clin Cancer Res 2002;8(1):221-32.

Singh P, Pandit S, Mokkapati VR, Garg A, Ravikumar V, Mijakovic I. Gold nanoparticles in diagnostics and therapeutics for human cancer. Int J Mol Sci 2018;19(7):1979.

Sharma H, Mishra PK, Talegaonkar S, Vaidya B. Metal nanoparticles: A theranostic nanotool against cancer. Drug Discov Today 2015;20(9):1143-51.

Chauhan A, Ranjan R, Avti P, Gulbake A. Tailoring the nanoparticles surface for efficient cancer therapeutics delivery. Int J Appl Pharm 2020:11-7.

Jeevanandam J, Barhoum A, Chan YS, Dufresne A, Danquah MK. Review on nanoparticles and nanostructured materials: history, sources, toxicity and regulations. Beilstein J Nanotechnol 2018;9(1):1050-74.

Mody VV, Siwale R, Singh A, Mody HR. Introduction to metallic nanoparticles. J Pharm Bioallied Sci 2010;2(4):282.

Singaravelan R, Alwar SB. Effect of reaction parameters in synthesis, characterisation of electrodeposited zinc nanohexagons. J Nanostruct Chem 2014;4:109-17.

Suwan T, Khongkhunthian S, Sirithunyalug J, Okonogi S. Effect of rice variety and reaction parameters on synthesis and antibacterial activity of silver nanoparticles. Drug Discov Ther 2018;12(5):267-74.

Mehravani B, Ribeiro AI, Zille A. Gold nanoparticles synthesis and antimicrobial effect on fibrous materials. Nanomaterials 2021;11(5):1067.

ISSN 2277-2685

IJPSL/May . 2022/ Vol-12/Issue-2/1-10